Bright and Water-Soluble Near IR-Emitting CdSe/CdTe/ZnSe Type-II/Type-I Nanocrystals, Tuning the Efficiency and Stability by Growth

Bridgette Blackman,[†] David Battaglia,[‡] and Xiaogang Peng*,[†]

Department of Chemistry & Biochemistry, University of Arkansas, Fayetteville, Arkansas 72701, and NN-Laboratories LLC, Fayetteville, Arkansas 72703

Received January 8, 2008. Revised Manuscript Received May 19, 2008

Highly photoluminescent CdSe/CdTe/ZnSe type-II/type-I composite nanocrystals, both dot- and peanut-shaped, were prepared via the modified successive ionic layer adsorption and reaction (SILAR) techniques, straight SILAR for peanut-shaped ones and SILAR coupled with thermal-cycling (SILAR-TC) for dot-shaped ones. The CdSe/CdTe type-II heterojunction offered the nanocrystals with near-infrared emission and the CdTe/ZnSe type-I heterojunction helped to confine the photogenerated charges away from the ligands and solution environment. This structural feature makes the photoluminescence quantum yield of the CdSe/CdTe/ZnSe core/shell/shell type-II/type-I dots that have a uniformly grown ZnSe shell retain as high as 60% after replacing the original amine ligands with mercaptopropionic acid (MPA). Conversely, the emission of the corresponding CdSe/CdTe core/shell dots (CdSe/CdTe/ZnSe composite peanuts) was completely (almost completely) quenched by the same ligand treatment. The emission properties of the MPA-coated CdSe/CdTe/ZnSe core/shell/shell dots were stable in water in the buffer solutions with their pH in a range between about 5 and 9.

Introduction

Colloidal semiconductor nanocrystals are being actively pursued as a class of new fluorescent materials in various fields, potentially for use as emitters in biomedical labeling,[1,2] quantum dot (QD)-based lasers,[3] and light-emitting diodes (LEDs).[4] They well-complement, and sometimes even compete favorably with, traditional organic dyes because of their high molar absorption extinction coefficient, tunability, emission color purity, broad excitation wavelength, unified synthetic chemistry for different colors, and photostability, etc. Among all of these potential applications, biomedical labeling is currently of great interest,[5] although it was introduced into the field only about 10 years ago.[1,2] For this specific application, nanocrystals emitting in the near-infrared (NIR) window, between 700 and 1000 nm, are of particular interest because of the well-known optical transparency of biological tissues in this window.[6] Built on the successful synthesis of CdSe/CdTe core/shell type-II quantum dots,[7] this report aimed to develop a class of efficient, stable, and water-soluble nanocrystals as NIR emitters. The basic nanocrystal structure is CdSe/CdTe/ZnSe core/shell/shell nanocrystals with an interior type-II heterojunction between CdSe and CdTe and a type-I heterojunction between CdTe and ZnSe. This kind of type-II/type-I composite nanocrystal system will be proven to be superior in comparison to the original type-II core/shell nanocrystals as NIR emitters in water. In this report, a type-I heterojunction refers to a junction formed by two different semiconductors, which confines both hole and electron in one of the semiconductors. Conversely, type-II heterojunction splits the photogenerated electron and hole into two different semiconductors.

NIR-emitting semiconductor nanocrystals in water potentially include two main classes. The first class is those semiconductor nanocrystals with a narrow bulk bandgap, such as InAs, PbSe, and CdTe, and their corresponding type-I core/shell nanocrystals. These nanocrystals are generally not ideal yet because of their inefficiency, instability, significant reabsorption/energy transfer, and/or poor ligand chemistry. The second class is type-II core/shell nanocrystals. Although the emission of type-II core/shell nanocrystals is spatially indirect, Bawendi's group[8] reported a significant emission efficiency for CdTe/CdSe core/shell type-II nanocrystals, about 4% photoluminescence (PL) quantum yield (QY), which is probably a result of the exceptionally large specific interface area for the core/shell nanocrystals. Inspired by this

* To whom correspondence should be addressed. Phone: (479) 575-4612. Fax: (479) 575-4049. E-mail: xpeng@uark.edu.
[†] University of Arkansas.
[‡] NN-Laboratories LLC.

(1) Bruchez, M., Jr.; Moronne, M.; Gin, P.; Weiss, S.; Alivisatos, A. P. *Science* **1998**, *281*, 2013–2016.
(2) Chan, W. C. W.; Nile, S. *Science* **1998**, *281*, 2016–2018.
(3) Klimov, V. I.; Mikhailovsky, A. A.; Xu, S.; Malko, A.; Hollingsworth, J. A.; Leatherdale, C. A.; Eisler, H.; Bawendi, M. G. *Science* **2000**, *290*, 314–7.
(4) Colvin, V. L.; Schlamp, M. C.; Allvisatos, A. P. *Nature* **1994**, *370*, 354–7.
(5) Michalet, X.; Pinaud, F. F.; Bentolila, L. A.; Tsay, J. M.; Doose, S.; Li, J. J.; Sundaresan, G.; Wu, A. M.; Gambhir, S. S.; Weiss, S. *Science* **2005**, *307*, 538–544.
(6) Kim, S.; Lim, Y. T.; Soltesz, E. G.; De Grand, A. M.; Lee, J.; Nakayama, A.; Parker, J. A.; Mihaljevic, T.; Laurence, R. G.; Dor, D. M.; Cohn, L. H.; Bawendi, M. G.; Frangioni, J. V. *Nat. Biotechnol.* **2004**, *22*, 93–97.
(7) Blackman, B.; Battaglia, D. M.; Mishima, T. D.; Johnson, M. B.; Peng, X. *Chem. Mater.* **2007**, *19*, 3815–3821.
(8) Kim, S.; Fisher, B.; Eisler, H.-J.; Bawendi, M. *J. Am. Chem. Soc.* **2003**, *125*, 11466–11467.

10.1021/cm8000688 CCC: $40.75
Published on Web 07/19/2008

initial work, extensive investigations have been directed toward type-II nanocrystals because of their NIR emission[7–13] for biomedical labeling as mentioned above.[6] It still remains a major challenge to produce water soluble nanocrystals with high PL QY that are stable for in vivo applications.

Through careful tailoring of the shell growth techniques, we have recently demonstrated quite improved PL QY as high as 30% for stable CdSe/CdTe core/shell nanocrystals.[7] This was achieved by coupling the successive ionic layer adsorption and reaction (SILAR) technique for growing colloidal core/shell nanocrystals[14] with a new concept of "thermal cycling" (SILAR-TC).[7] SILAR-TC allowed us to control uniform epitaxial growth of the shell material onto the existing nanocrystals, forming dot-shaped core/shell nanocrystals with monolayer-controlled thicknesses of the CdTe shell vs peanut-shaped nanocrystals with a CdSe−CdTe heterojunction. In the latter case, the CdTe growth was found to be predominantly at the end(s) of the core nanocrystals. In attempts to further boost the PL QY, type-II heterojunctions were examined using both quantum dots and quantum shell nanocrystals as the starting materials for the formation of the type-II nanocrystals, each of which was tested with a variety of shell thicknesses and sizes.[7] In all of these attempts, one interesting point is that straight SILAR always ended up either with minimum growth of the shell or forming peanut-shaped heterojunction nanocrystals, and SILAR-TC yielded the type-II core/shell dots or core/shell/shell type-I/type-II dots. Unfortunately, 30% PL QY was about the highest for stable dots, however up to 50% PL QY was observed for unstable ones. More importantly, these quite emissive nanocrystals were found to not emit at all after they were modified by hydrophilic thiol ligands for dispersion in aqueous solutions as to be described below.

The present report shall demonstrate that it is possible to simultaneously meet high efficiency, high stability, and water-dispersibility for the CdSe/CdTe core/shell type-II nanocrystals with NIR emission. The solution comes from the additional epitaxial growth of several monolayers of ZnSe onto the CdSe/CdTe core/shell nanocrystals. The additional ZnSe shell, with a substantially wide bulk bandgap comparing to both CdSe and CdTe, serves to form a type-I heterojunction with the CdTe layer, thus efficiently confining both electrons and holes within the CdSe/CdTe structure and substantially enhancing the spatial indirect radiative recombination at the CdSe core and inner CdTe shell interface. Experimental results again reveal that SILAR-TC is a viable technique for the controlled and uniform deposition of the shell (both CdTe and ZnSe ones) onto the existing nanocrystals in solution. Not surprisingly, the emission properties were found to be significantly more durable for the dot-shaped type-II/type-I composite nanocrystals than for the corresponding peanut-shaped ones. For instance, after ligand exchange with hydrophilic thiol ligands, the CdSe/CdTe/ZnSe type-II/type-I dots was made to be water soluble without sacrificing their high PL QY and solution stability.

Experimental Section

Chemicals. Cadmium oxide (99.99%), zinc oxide (99.9%), selenium (99.5%, 100 mesh), tellurium (99.8%, 325 mesh), tributylphosphine (TBP, 97%), 1-octadecene (ODE), oleic acid (OA, 90%), benzoyl peroxide, oleylamine (70%), 3-mercaptopropionic acid (MPA, 99 +%), and sodium bicarbonate were purchased from Aldrich. IR-125 dye was purchased from Exciton. The CdSe cores were from NN-Laboratories and prepared through the known "greener methods" for nanocrystal synthesis.[15] All organic solvents were purchased from EM Sciences. All chemicals were used directly without any further purification unless otherwise stated.

Preparation of Cd, Te, Se, and Zn Precursor Solutions. The Cd, Te, and Se precursor solutions were prepared following procedures previously reported by our group.[7] Namely, the Cd precursor solution (0.04 M) was prepared by adding CdO (0.05 g) and oleic acid (0.90 g) in a 1:8 molar ratio to a 25 mL 3-neck round-bottomed flask followed by 7.08 g of octadecene (ODE). The CdO mixture was sealed, purged with argon, and then heated to 240 °C until the solution turned clear. After being cooled to ~60 °C, the Cd precursor solution (0.04 M) was transferred to a 20 mL glass vial capped with a rubber septum and stored at room temperature. In a glovebox, the Te precursor (0.04 M) was prepared by adding pure Te powder (0.06 g) to a 20 mL glass vial which was then dissolved in tributylphoshine (TBP, 1.55 g) at a 1:16 molar ratio. ODE (7.95 g, degassed) was then added and the mixture was capped with a rubber septum, removed from the glovebox, sonicated, and if necessary, heated up to 100 °C to dissolve any remaining Te. The Se precursor solution (0.04 M) was prepared similarly to the Te precursor solution in a glovebox. Pure Se powder (0.38 g) was dissolved in TBP (1.55 g, 1:16 molar ratio) and ODE (7.95 g, degassed) in a 20 mL glass vial and capped with a rubber septum. The Zn precursor solution (0.04 M) was prepared by combining ZnO (0.03 g) and oleic acid (0.90 g) in a 1:8 molar ratio with ODE (7.08 g) inside a 25 mL 3-neck round-bottomed flask equipped with a stir bar. The ZnO mixture was capped with a rubber septum, purged with argon, and then heated to 250 °C with constant stirring until the solution turned clear. After being cooled to ~60 °C, the solution was placed in a 20 mL glass vial capped with a rubber septum and stored at room temperature.

SILAR Synthesis of CdSe/CdTe/ZnSe Core/Shell/Shell Dots by SILAR-TC. For a typical synthesis, to a 25 mL 3-neck round-bottomed reaction flask equipped with a stir bar were added 3.0 g of oleylamine and 3.0 g of ODE. About 2.5×10^{-5} mmol of CdSe core nanocrystals (4.8 nm) in hexanes was also added to the flask. The flask was then put under a vacuum for the removal of air and hexanes while heating to 100 °C with constant stirring. The reaction was purged with argon for at least 10 min and further heated to 190 °C. The Cd and Te precursor solutions (0.14 mL each) were added consecutively via syringe to the reaction flask containing the CdSe cores, waiting 5 min between each injection. The temperature was increased immediately to 250 °C for 20 min to allow growth of the first CdTe monolayer, and then decreased back to 190 °C. Next, 0.18 mL of the Cd and Te precursor solutions were injected as before using the same time intervals and temperature changes for growth of a second CdTe monolayer.

(9) Balet, L. P.; Ivanov, S. A.; Piryatinski, A.; Achermann, M.; Klimov, V. I. *Nano Lett.* **2004**, *4*, 1485–1488.
(10) Li, J. J.; Tsay, J. M.; Michalet, X.; Weiss, S. *Chem. Phys.* **2005**, *318*, 82–90.
(11) Yu, K.;; Zaman, B.;; Romanova, S.;; Wang, D.-s.;; Ripmeester, J. A. *Small* **2005**, *1*, 332–338.
(12) Halpert, J. E.; Porter, V. J.; Zimmer, J. P.; Bawendi, M. G. *J. Am. Chem. Soc.* **2006**, *128*, 12590–12591.
(13) Wang, C. H.; Chen, T. T.; Tan, K. W.; Chen, Y. F.; Cheng, C. T.; Chou, P. T. *J. Appl. Phys.* **2006**, *99*, 123521/1–123521/4.
(14) Li, J. J.; Wang, Y. A.; Guo, W.; Keay, J. C.; Mishima, T. D.; Johnson, M. B.; Peng, X. *J. Am. Chem. Soc.* **2003**, *125*, 12567–12575.
(15) Qu, L.; Peng, X. *J. Am. Chem. Soc.* **2002**, *124*, 2049–2055.

Without further purification, the temperature was raised to 250 °C for layering of the ZnSe shell. Two monolayers of the ZnSe shell were grown onto the CdSe/CdTe nanocrystals by adding 0.33 mL (1st layer) and 0.41 mL (2nd layer) of the Zn and Se precursor solutions, sequentially. After the injections of the precursor solutions took place at 250 °C, the temperature was immediately increased to 310 °C initiating the shell growth. Cycling of the injection and growth temperatures continued for both the first and second monolayers of the ZnSe shell. Aliquots (~1 mL) were taken between each injection to monitor the shell growth. Upon completion of the synthesis, the reaction was cooled down to ~70 °C, transferred to a 20 mL vial, and diluted with acetone until the solution became cloudy (indicating nanocrystal precipitation). The precipitate was spun down in a centrifuge at 3000 RPM for 10 min, the supernatant was then decanted, and the resulting nanocrystals were diluted with 1−2 mL of toluene.

SILAR Synthesis of CdSe/CdTe/ZnSe Peanut-Shaped Composite Nanocrystals. For a typical synthesis, the CdSe/CdTe dots were prepared as described in the synthesis above. After growth of the dots at 250 °C, the Zn and Se precursor solutions (0.33 mL each) were added consecutively via syringe to the reaction flask, waiting 5 min between each injection. The temperature was kept at 250 °C for 20 min to allow growth of the first ZnSe layer, followed by a second addition of 0.41 mL of Zn and Se precursor solutions for the second monolayer. The reaction was allowed to cool to ~70 °C and the peanuts were then purified and isolated as described for the dots above.

Ligand Exchange of CdSe/CdTe/ZnSe Nanocrystals..[16] Approximately 2 mL of purified CdSe/CdTe/ZnSe nanocrystals in toluene were diluted to 4 mL with chloroform, followed by addition of MPA until the solution became cloudy. The mixture was then shaken for 20 min and the MPA-capped CdSe/CdTe/ZnSe nanocrystals were flocculated, separating out the nanocrystals from the free MPA, which remained dissolved in the chloroform. Repeated centrifugations in chloroform were used to remove free MPA from the mixture. Finally, the desired amount of water (or buffer) was added to the precipitated nanocrystals, and sodium bicarbonate was added until the nanocrystals were completely dissolved in the water. In cases where buffer solutions were used, the addition of sodium bicarbonate was not necessary.

Transmission Electron Microscopy (TEM). The TEM images were taken on a JEOL 100CX transmission electron microscope with an acceleration voltage of 80 kV. All samples were purified by acetone precipitation from a chloroform solution or hexanes/methanol extraction. Either Formvar film- or ultrathin carbon film-coated copper grids were dipped in the hexanes or toluene solutions to deposit nanocrystals onto the film. Randomly oriented nanocrystals on the TEM substrate were obtained using a diluted nanocrystal solution, with an absorbance of the first absorption peak of the nanocrystals below about 0.05. If the absorbance was above 0.2, densely packed monolayers and multilayers of nanocrystals were observed. Selected area electron diffraction patterns (SAED) were taken with a camera length of 120 cm.

Optical Measurements. Absorption spectra were measured on a HP 8453 diode array spectrophotometer. Photoluminescence was measured on a Spex Fluorolog 3−111 using a PMT detector for spectra between 200 and 800 nm and a liquid-nitrogen-cooled InGaAs photodiode detector for emission in the NIR (650−1600 nm). Photoluminescence quantum yields (PL QY) of the samples were determined through comparison using an IR-125 standard organic dye with the excitation wavelength set at 740 nm. All samples for measurements consisted of nanocrystals dissolved in 1 mL of solvent.

Etching of CdSe/CdTe/ZnSe Nanocrystals. Etching of the dots and peanuts with different compositions were carried out in the same manner as our previous reports.[7,17] For a typical process, 1.0 mL of benzylamine was added to 0.5 mL of the purified CdSe/CdTe/ZnSe dots or peanuts, and the resulting suspension was sonicated for 20 min until the mixture turned clear. (This allowed time for an exchange of the ODA surface ligands with benzylamine.) Subsequently, 0.2 mL of the sonicated CdSe/CdTe/ZnSe nanocrystal solution was transferred to a 1 mL quartz cuvette, equipped with a micro stir bar, followed by 0.2 mL of methanol and 0.3 mL of toluene. The cuvette was sealed, placed in a UV−vis sample holder, and stirred. To initiate the etching process, 0.1 mL of a 0.2 M benzoyl peroxide solution in toluene/methanol (4:1) was added to the cuvette by syringe. During this process, the absorption of the nanocrystals was monitored in real time at range of 400−800 nm for up to 200 s using an Ocean Optics USB2000 UV−vis spectrometer.

Results and Discussion

ZnSe shell growth onto CdSe/CdTe core/shell nanocrystals was developed on the basis of the synthesis of CdSe/CdTe core/shell nanocrystals, which we reported recently.[7] As mentioned above, attempts to generate water-soluble CdSe/CdTe core/shell nanocrystals failed. This is probably because of the hole trapping by the negatively charged thiolate ligands bounded on the surface of the CdTe shell.[18] This possible mechanism implies that if a wide bandgap semiconductor can be epitaxially grown onto the outer surface of the CdSe/CdTe core/shell dots to further form an additional type-I interface with CdTe (Figure 1), this quenching problem should be solved. Following this assumption, ZnSe was chosen. As shown in Figure 1, the bulk conduction band (valence band) of ZnSe is higher (lower) than the conduction band (valence band) of both CdSe and CdTe, which should offer an excellent confinement for both photogenerated electrons and holes. Compared to another zinc chalcogenide semiconductor with a wide bandgap, ZnS, the lattice of ZnSe is much closer to that of CdTe.

The epitaxial growth conditions for the CdSe/CdTe/ZnSe core/shell/shell nanocrystals were found to be somewhat similar to that of the CdSe/CdTe core/shell nanocrystals. When the SILAR technique for colloidal nanocrystals[14] was applied alone, growth of peanut-shaped CdSe/CdTe/ZnSe nanocrystals (Figure 2, bottom left) was possible at a fixed temperature (see Experimental Section for details). The SILAR-TC technique allowed the growth of dot-shaped core/shell/shell nanocrystals (Figure 2, bottom right) with a similar size distribution of the initial CdSe/CdTe core/shell nanocrystals (Figure 2, middle). The difference in growth patterns for two different growth techniques is discussed below through a typical reaction.

The TEM pictures in Figure 2 are related to a specific experiment with 4.8 nm CdSe nanocrystals as the core. Prior to the growth of the ZnSe shell, 2 monolayers of CdTe were

(16) Pradhan, N.; Battaglia, D. M.; Liu, Y.; Peng, X. *Nano Lett.* **2007**, *7*, 312–317.
(17) Battaglia, D.; Blackman, B.; Peng, X. *J. Am. Chem. Soc.* **2005**, *127*, 10889–10897.
(18) Aldana, J.; Wang, Y. A.; Peng, X. *J. Am. Chem. Soc.* **2001**, *123*, 8844–8850.

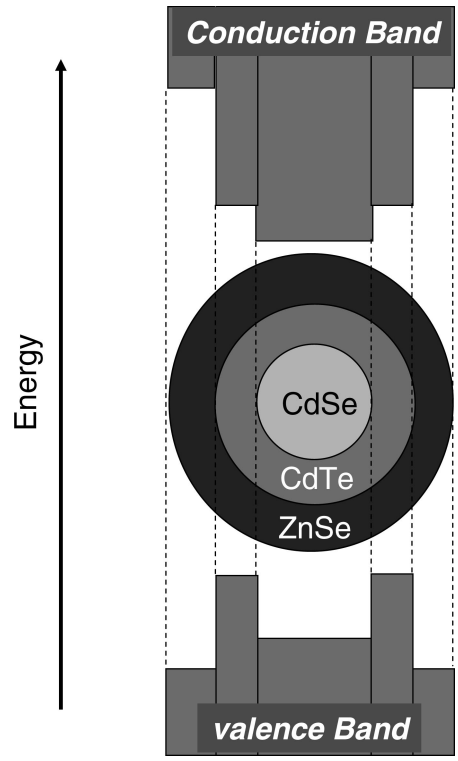

Figure 1. Schematic illustrateion of the bulk band offsets of CdSe/CdTe/ZnSe type-II/type-I heterostructures.

grown onto the core using the reported method, either SILAR or SILAR-TC. At first, the SILAR-TC method[7] yielded dot-shaped CdSe/CdTe core/shell type-II nanocrystals with the average size as about 6 nm (Figure 2, middle), which were used as the starting materials for both CdSe/CdTe/ZnSe type-II/type-I dots and peanuts. The last step attempted to grow the ZnSe outer shell (targeting two monolayers of ZnSe shell) onto these type-II core/shell dots. When the growth was performed with the SILAR-TC technique, the resulting CdSe/CdTe/ZnSe complex nanocrystals were nearly dot shaped (Figure 2, bottom right), and the slight elongation might be a result of the intrinsic properties of II−VI nanocrystals.[19] The average size of the resulting CdSe/CdTe/ZnSe core/shell/shell nanocrystals was about 8 nm, which reasonably matched the expected size increase.

When the SILAR technique without "thermal cycling" was applied, the resulting nanocrystals were peanut-shaped (Figure 2, bottom left). The dimension of the short axes of the peanuts in Figure 2 (bottom left) was approximately the same as the diameter of the CdSe/CdTe core/shell dots (Figure 2, middle) and the aspect ratio was about 2 in average. This implies that the growth of ZnSe was not uniform and, along the short axes, the CdSe/CdTe core/shell dots might be barely coated by ZnSe. This structural feature greatly affected the etching pattern and the durability of the resulting nanocrystals to be discussed below. As reported previously, the peanuts were likely formed because of the low reactivity of the precursors, which produced a buildup of monomers on the unique axis.[7,20] In spite of their shape difference between dots and peanuts (Figure 2, bottom), the crystal structure of both types of the CdSe/CdTe/ZnSe complex nanostructures revealed by the selected area electron diffraction patterns (SAED) resembled that of a mixed wurtzite and zinc-blend structure, which was the crystal structure of the core nanocrystals.[19]

The optical properties, both absorption and emission spectra, for the CdSe/CdTe/ZnSe dots and peanuts were similar. Figure 3 displays the UV−vis, PL, and PLE obtained during the growth of the CdSe/CdTe/ZnSe core/shell/shell dots at different stages. Before the growth of either CdTe or ZnSe shells, the UV−vis spectrum was a typical CdSe quantum dot sample with nearly monodisperse size distribution, sharp distinctive peaks between 450−650 nm (Figure 3, bottom spectra). After growth of two monolayers of the CdTe shell (Figure 3, middle), it was replaced by a spectrum without distinguishable absorbance peaks but with a featureless and long absorption tail at lower energies (between 650 and 700 nm). The long tail and the smeared absorption peaks are considered as a signature of the spatial indirect absorption of the type-II heterojunction in a nanocrystal.[7,8] Upon the growth of the additional ZnSe shell (Figure 3, top), no substantial change in the absorption band edge was observed, although a slight broadening between 550 and 750 nm was observed. This was expected because ZnSe has a very wide bulk band gap in comparison to CdTe that forms the type-I junction with the ZnSe shell.

Relative to the CdSe core, a substantial red-shift of the emission peak to a window between 850 and 1000 nm was observed in the photoluminescence (PL) spectra during the growth of the CdTe shell (Figure 3, middle). This observation, being typical for type-II systems,[8] was due to the spatially indirect recombination of the charge carriers at the type-II heterojunction. The PL still remained in the NIR window for the ZnSe shell growth, shifting slightly to the red (850−1100 nm) for the experiment corresponding to Figure 3. The exact reason for this slight red-shift is not clear, but it might be a result of the compressed lattice for CdSe and CdTe due to the growth of the ZnSe shell.

As expected, the PL QY of the type-II emission was greatly enhanced upon the growth of the ZnSe shell. For the specific experiment related to Figure 3, the PL QY of the CdSe/CdTe core/shell type-II dots was about 20%. Upon the growth of the ZnSe shell, it increased to about 50 and 60% for the resulting peanuts and dots, respectively. This indicates that, for the CdSe/CdTe/ZnSe peanuts, even though the ZnSe shell was not completely uniform in the growth, some surface coating by ZnSe shell did occur for the entire CdSe/CdTe dots in this type of elongated products. Different from the high PL QY (around 50%) CdS/CdSe/CdTe core/shell/shell type-I (quantum well)/type-II dots with a thin CdTe layer,[7] these highly bright type-II/type-I complex nanocrystals, both dots and peanuts, can withstand purification and storage in solvents (see more detail below).

Different from plain cores and type-I core/shell dots, lack of distinguishable absorption peaks in type-II nanocrystals may not reflect a broad size distribution of the nanocrystals because of their spatial indirect absorption transitions.[7] A qualitative and simple way to clear out this is to compare

(19) Murray, C. B.; Norris, D. J.; Bawendi, M. G. *J. Am. Chem. Soc.* **1993**, *115*, 8706–15.
(20) Peng, X.; Thessing, J. *Struct. Bonding* **2005**, *118*, 79–119.

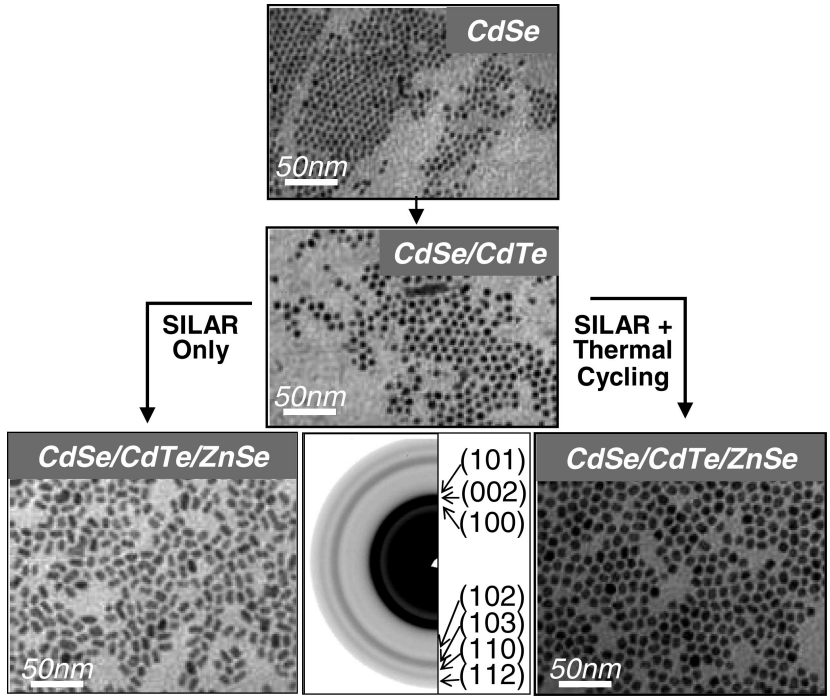

Figure 2. TEM images and SAED patterns throughout the growth of CdSe/CdTe/ZnSe dots and peanuts synthesized from the SILAR reaction under different temperature conditions.

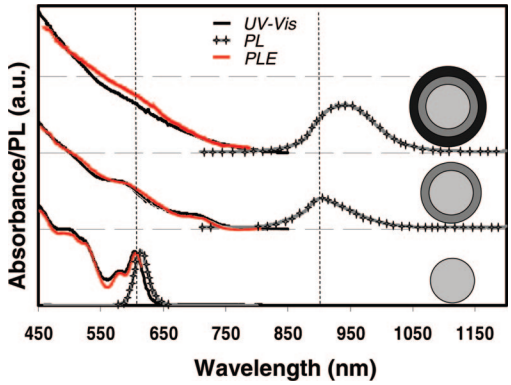

Figure 3. UV−vis, PL, and PLE spectra for the evolution of the growth of the NIR-emitting CdSe/CdTe/ZnSe dots. Two monolayers of the inner CdTe (middle spectra) and outer ZnSe (top) shells were grown onto the CdSe cores (bottom).

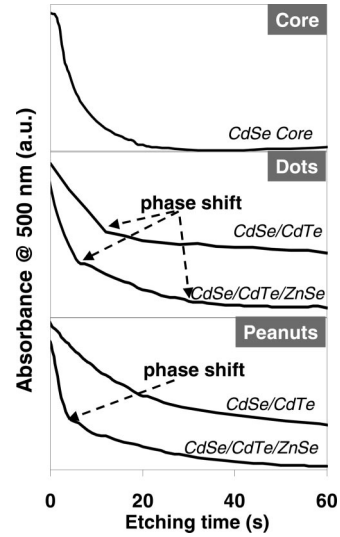

Figure 4. Oxidative etching of nanocrystals with different compositions and shapes monitored at 500 nm.

the absorption spectrum and the corresponding photoluminescence excitation (PLE) spectrum. Because the emission is fixed at a given wavelength, only those nanocrystals that give the emission at the given wavelength shall contribute to the PLE. Consequently, PLE reflects the absorption properties of a selected subset of nanocrystals in a given sample if the sample has a broad size distribution. For all three samples in Figure 3, namely, CdSe core, CdSe/CdTe core/shell dots, and CdSe/CdTe/ZnSe type-II/type-I dots, the PLE spectra (monitored at different wavelengths for a given sample) closely matched the corresponding absorption spectrum. This is consistent with the nearly monodisperse size distribution of all three samples as revealed by TEM measurements (Figure 2).

ZnSe shell growth was confirmed by controlled oxidative etching methods to rule out alloying (Figure 4). This etching method[7,17] relied on the irreversible etching of the chalcogenides in a controlled fashion by a benzoyl peroxide solution. The etching process was monitored in situ using a UV−vis spectrometer.[7,17] The temporal evolution of the absorption properties during etching can be illustrated by either the entire absorption spectrum range[7,17] or the absorbance at a single wavelength.[21] In principle, as atoms were removed from the surface of the nanocrystals, the nanocrystals shall experience some abrupt changes of the optical properties at the interface. If the materials at the interface were significantly alloyed, such abrupt changes should disappear because the interface was smeared.

(21) Ivanov, S. A.; Piryatinski, A.; Nanda, J.; Tretiak, S.; Zavadil, K. R.; Wallace, W. O.; Werder, D.; Klimov, V. I. *J. Am. Chem. Soc.* **2007**, *129*, 11708–11719.

Relevant to this work, the most interesting interface was the one between ZnSe and CdTe. As shown in Figure 3, the absorption spectra of the nanocrystals with/without the ZnSe shell actually did not show substantially different structures. However the chemical reactivity of the ZnSe and CdTe toward the oxidant, oxidation of Se^{2-} vs Te^{2-}, should be significantly different. For this reason, monitoring the etching process at a given wavelength (500 nm), instead of the broad absorbance spectral range, may better serve the purpose. Figure 4 displays the time-dependence of the absorbance at 500 nm for the plain CdSe cores, CdSe/CdTe and CdSe/CdTe/ZnSe dots and peanuts.

The etching of pure CdSe core nanocrystals (Figure 4, top) showed a smooth decrease pattern of the absorbance without an abrupt turning point that is labeled as "phase shift" for the core/shell structures[21] (Figure 4, middle and bottom). The two samples in the middle panel in Figure 4 were two dot-shaped samples, i.e., CdSe/CdTe core/shell dots and CdSe/CdTe/ZnSe core/shell/shell dots. The CdSe/CdTe core/shell dots (with four monolayers of CdTe) experienced a "phase shift" in the etching process, which indicates the etching was going through the CdSe-CdTe interface.[7,17,21] The CdSe/CdTe/ZnSe core/shell/shell dots (Figure 4, middle), experienced two "phase shift" points. Presumably, the two monolayers of ZnSe shell disappeared rapidly upon the etching, which resulted in the first transition point. The second "phase shift", which is less obvious, should be a result of the transition from the CdTe shell to the CdSe core.

The two etching curves in the bottom panel of Figure 4 are associated with peanut-shaped CdSe/CdTe and CdSe/CdTe/ZnSe complex nanostructures. The comparative CdSe/CdTe peanuts did not show two phases, which is consistent with our early results. As we reported previously, the CdSe/CdTe peanuts were basically composed of two distinguishable ends, one end being CdSe and the other being CdTe. In earlier etching experiments, a noticeable type-II tail was still observed for the CdSe/CdTe peanuts when the particles reached the size of the original CdSe cores.[7] Equivalently, because both CdSe and CdTe sections were etched simultaneously, no "phase shift" should be expected when the data were presented by single-wavelength absorption (Figure 4, bottom panel). On the contrary, the CdSe/CdTe/ZnSe peanuts did exhibit a clear "phase shift". Therefore, there was indeed a ZnSe shell deposition onto the CdSe/CdTe composite nanocrystals, which is consistent with the enhanced PL QY of the CdSe/CdTe/ZnSe peanuts in comparison to the CdSe/CdTe core/shell nanocrystals as described above. However, in comparison with the corresponding CdSe/CdTe/ZnSe dots with the same amount of ZnSe deposition, the "phase shift" for the CdSe/CdTe/ZnSe peanuts was much earlier, about half of the time for the peanuts sample. This implies that, under parallel conditions, the oxidative etching reached the CdTe layer much easier for the CdSe/CdTe/ZnSe peanuts than that for the CdSe/CdTe/ZnSe core/shell/shell dots. For the dots, the ZnSe shell was about two monolayers for the sample in Figure 4 (middle). Thus, the thickness of the thin parts of the ZnSe shell on the CdSe/CdTe/ZnSe peanuts should be roughly one monolayer or less.

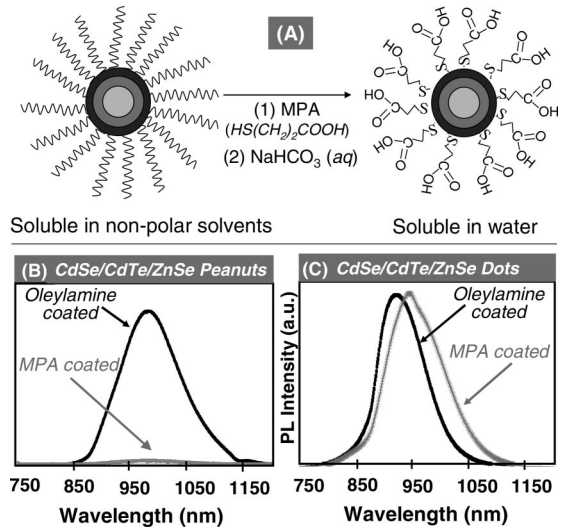

Figure 5. (A) Schematic representation of a ligand-exchange process to generate water soluble type-II/type-I composite quantum dots. (B, C) PL spectra of MPA- and oleylamine-coated CdSe/CdTe/ZnSe peanuts (B) and dots (C). MPA coated nanocrystals were dispersed in water. Oleylamimine-coated nanocrystals were in toluene.

Water-soluble samples of both CdSe/CdTe/ZnSe complex nanocrystals dots and peanuts were prepared by replacing the original hydrophobic oleylamine ligands obtained in the synthesis with 3-mercaptopropionic acid (MPA) (Figure 5A). The deprotonated thiol group (thiolate) is known to be a strong bonding group to the surface cations of II−VI and III−V nanocrystals, which has thus been widely used for their surface ligand replacement. However, thiolates are known to completely quench the photoluminescence of CdSe and ZnSe plain core nanocrystals.[18] To avoid this quenching, we should coat the regular plain core semiconductor nanocrystals by a shell that has a wide bandgap and a reasonable thickness.

Thiolates are thought to quench PL of semiconductor nanocrystals by acting as surface hole traps. Evidently, this is consistent with the complete quenching of the PL of CdSe/CdTe core/shell type-II dots. This is so because the CdTe shell should actually bring the photogenerated holes more close to the surface although it does confine the electrons into the core (see the band alignments between CdSe and CdTe in Figure 1).

If the ZnSe was grown onto the CdSe/CdTe core/shell dots nonuniformly to form peanuts, the resulting CdSe/CdTe/ZnSe composite nanocrystals were still quite sensitive to the thiolate coating. In Figure 5 (B), the PL was largely quenched after the original oleylamine ligands were replaced by MPA, from about 50% down to less than 10%. This is consistent with the structural results revealed by TEM (Figure 2) and etching experiments (Figure 4), that the ZnSe shell was not uniform and some parts of the CdSe/CdTe/ZnSe peanuts would only have roughly one-monolayer of the ZnSe coating.

The PL brightness of the CdSe/CdTe/ZnSe core/shell/shell dots, however, was insensitive to the thiolate ligands (Figure 5C). The PL QY maintained about the same emission level after the ligand exchange, about 50−60%, before and after the ligand exchange (see Figure 5). This is consistent with the uniform coating of the ZnSe shell onto the CdSe/CdTe

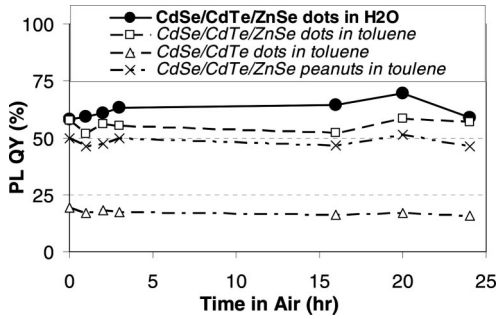

Figure 6. PL QY stability of water-soluble CdSe/CdTe/ZnSe dots and PL QY of CdSe/CdTe and CdSe/CdTe/ZnSe nanocrystals in toluene over a 24 h period.

core/shell dots. In other words, the type-I band offsets between the CdTe and ZnSe layers effectively confined the photogenerated holes into the CdTe shell. Based on the overall band offsets in Figure 1, the photogenerated electrons should be funneled into the CdSe core with the type-II and type-I heterojunctions. Interestingly, the PL emission peak position shifted to red slightly after the MPA ligand exchange. At this moment, we do not know the exact reason.

Stability of the water soluble CdSe/CdTe/ZnSe type-II/type-I emitters was tested briefly under common solution conditions. Earlier studies on quantum dots coated with MPA ligands indicated that such nanocrystals were unstable because of the extremely small size of MPA,[18] which often resulted in a rapid precipitation of the nanocrystals from the water solution upon exposure to ambient light and air. The stability of the emission properties of the MPA-coated CdSe/CdTe/ZnSe core/shell/shell dots in water was monitored under ambient conditions, in air and room light, for 24 h (Figure 6). The results indicate that, at least under such ambient conditions, the PL properties of the MPA-coated CdSe/CdTe/ZnSe core/shell/shell dots in water were stable. The fluctuation of the PL QY values of the MPA-coated CdSe/CdTe/ZnSe core/shell/shell dots in Figure 6 are believed to be a result of the experimental errors. As shown in the Figure, the three control samples, all of them in toluene, experienced a similar fluctuation trend. These control experiments further indicate an acceptable stability of the purified and highly emissive CdSe/CdTe/ZnSe composite nanocrystals, both dots and peanuts, in the solvents under ambient conditions. Conversely, the high PL QY (around 50%) CdS/CdSe/CdTe core/shell/shell type-I (quantum well)/type-II dots with a thin CdTe layer, was found to be unstable under similar conditions.[7]

The PL properties of the water-soluble MPA-coated CdSe/CdTe/ZnSe core/shell/shell dots were also briefly examined in different buffers (data not shown). In summary, in the pH range between about 5 and 9, the emission properties of the nanocrystals were not very much affected. The nanocrystals were also found to be tolerant of salt, 0.1−1.0 mol/L NaCl aqueous solutions, although the particles are believed to be negatively charged because of the carboxylate groups of MPA ligands.

Conclusions

The PL efficiency and stability of CdSe/CdTe core/shell type-II dots were both improved by the growth of a wide bandgap semiconductor (ZnSe) onto the CdTe surface. This is so because a type-I heterojunction between CdTe and ZnSe layers confined the photogenerated electrons and holes within CdSe and CdTe, respectively. It was found to be important to control the uniform growth of the ZnSe shell onto the CdSe/CdTe core/shell dots to achieve optimal efficiency and stability. The uniform growth of the ZnSe shell was made possible by SILAR-TC technique. Although MPA quenched the PL of CdSe/CdTe core/shell dots completely and dimmed the PL of the CdSe/CdTe/ZnSe peanuts, the PL QY of CdSe/CdTe/ZnSe core/shell/shell dots did not decrease upon the MPA coating. The bright MPA-coated CdSe/CdTe/ZnSe core/shell/shell dots, with PL QY as high as being around 50−60% in water, were found to be stable for at least 24 h under ambient conditions. These bright and water-soluble type-II/type-I dots were also found to be compatible with buffer solutions (pH being around 5−9) and a substantial ionic strength (NaCl concentration being 0.1−1.0 mol/L). These results indicate that these highly luminescent, water-soluble nanocrystals could potentially be useful in biomedical imaging. The near-infrared emission color may make them especially interesting for in vivo imaging applications.[6]

Acknowledgment. Financial support from the NIH, NSF, and Arkansas Biomedical Institute is acknowledged.

CM8000688